Supplemental Figures to:

# Identification and validation of larixyl acetate as a potent TRPC6 inhibitor

Nicole Urban, Liming Wang, Sandra Kwiek, Jörg Rademann,
Wolfgang M. Kuebler, and Michael Schaefer

**Molecular Pharmacology**

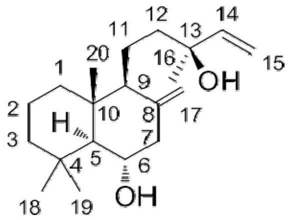


**Supplemental Figure 1: Structure and chemical characterisation of Larixol**

**$R_f$** = 0.02 (Hexan: EE 9:1 (v:v)

**$T_m$** = 100°C

**$^{1}$H-NMR** (300 MHz, $CDCl_3$) δ [ppm] = 0.68 (s, 3H, 20- C**$H_3$**), 0.99 (s, 3H, 18/19-C**$H_3$**), 1.01-1.60 (m, 12H), 1.16 (s, 3H, 18/19-C**$H_3$**), 1.13 (d, 1H, 5-C**H**), 1.26 (s, 3H, 16-C**$H_3$**), 2.04 (t, 1H, 7-C**H**), 2.66 (dd, 1H, 7-C**H**), 3.82 (dt, 1H, 6-C**H**), 4.65 (dd, 2H, 17- C**$H_2$**), 5.04 (dd, 1H, 15-C**H**, $J_{cis}$ = 10.37 Hz, $J_{geminal}$ = 1.26 Hz), 5.18 (dd,1H, 15-C**H**, $J_{trans}$ = 17.37 Hz, $J_{geminal}$ = 1.26 Hz), 5.89 (dd, 1H, 14-C**H,** $J_{trans}$ = 17.37 Hz, $J_{cis}$ = 10.37 Hz)

**$^{13}$C-NMR** (75 MHz, $CDCl_3$) δ [ppm] = 16.3 (20-**C**$H_3$), 18.3 (11-**C**$H_2$), 19.4 (2-**C**$H_2$), 22.6 (18/19-**C**$H_3$), 28.0 (16-**C**$H_3$), 34.1 (4-**C**), 36.9 (18/19-**C**$H_3$), 39.6 (1-**C**$H_2$), 39.8 (10-**C**$H_2$), 41.6 (12-**C**$H_2$), 44.0 (3-**C**$H_2$), 49.4 (7-**C**$H_2$), 56.7 (9-**C**H), 60.8 (5-**C**H), 71.9 (6-**C**H), 73.8 (13-**C**), 108.6 (17-**C**$H_2$), 111.9 (15-**C**$H_2$), 145.4 (14-**C**H), 145.8 (8-**C**)

**HRMS** [$M+Na^+$] calculated 329.24565 Da, found 329.24510 m/z.

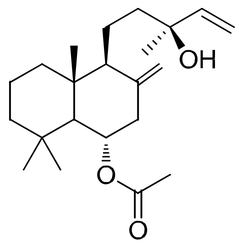

**Supplemental Figure 2: Structure and chemical characterisation of larix-6-yl monoacetate**

$\mathbf{R_f}$ = 0.30 (Hexan: EE 4:1(v:v))

**$^{1}$H-NMR** (300 MHz, $CDCl_3$) δ [ppm] = 0.73 (s, 3H, 20- C**$H_3$**), 0.83 (s, 3H, 18/19-C**$H_3$**), 1.00 (s, 3H, 18/19-C**$H_3$**), 1.03-1.80 (m, 12H), 1.26 (s, 3H, 16-C**$H_3$**), 1.40 (d, 1H, 5-C**H**), 2.02 (s, 3H, Ac-C**$H_3$**), 2.66 (dd, 1H, 7-C**H**), 4.63 (m, 1H, 17-C**$H_2$**),), 4.91 (m, 1H,17-C**$H_2$**), 4.97-5.06 (m, 2H,), 5.19 (dd,1H, 15-C**H**), 5.89 (dd, 1H, 14-C**H**)

**$^{13}$C-NMR** (75 MHz, $CDCl_3$) δ [ppm] = 16.2 (20-**C**$H_3$), 18.2 (11-**C**$H_2$), 19.2 (2-**C**$H_2$), 22.2 (Ac-**C**$H_3$), 22.7 (18/19-**C**$H_3$), 28.0 (16-**C**$H_3$), 33.7 (4-**C**), 36.4 (18/19-**C**$H_3$), 39.3 (1-**C**$H_2$), 40.1 (10-**C**$H_2$), 41.5 (12-**C**$H_2$), 43.7 (3-**C**$H_2$), 44.4 (7-**C**$H_2$), 56.6 (9-**C**H), 57.8 (5-**C**H), 73.5 (6-**C**H), 73.7 (13-**C**), 109.7 (17-**C**$H_2$), 111.9 (15-**C**$H_2$), 144.5 (14-**C**H), 145.4 (8-**C**), 170.3 (Ac-**C**O)

**HRMS** [$M+Na^+$] calculated 371.25621 Da, found 371.25567 m/z

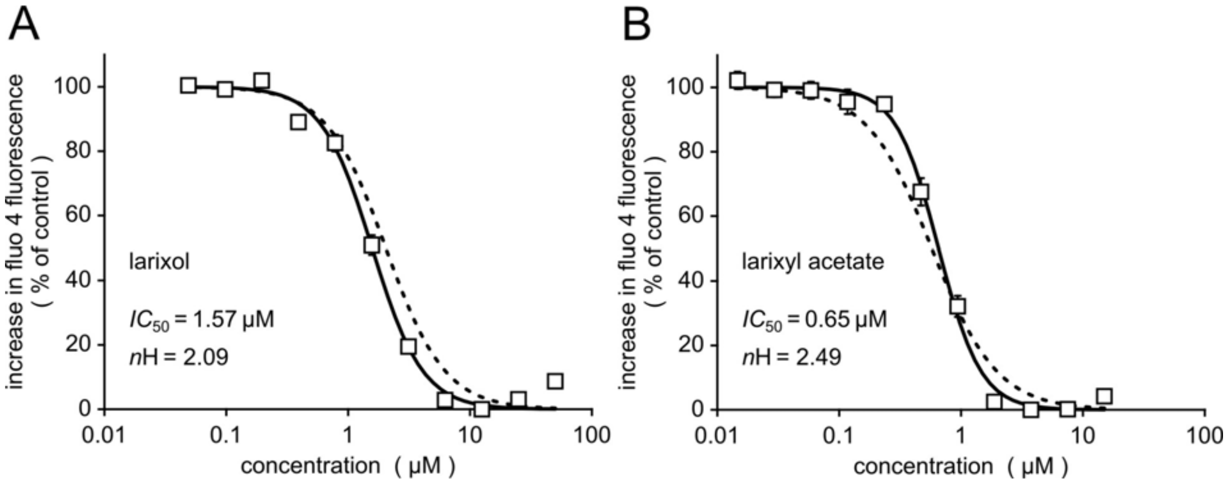


**Supplemental Figure 3: Potency of larixol and larixyl acetate to inhibit $Ca^{2+}$ entry through TRPC6 in the receptor-induced mode of activation.**

To assess whether the TRPC6 inhibitors are effective when TRPC6 is activated in a receptor-mediated fashion, fluo-4-loaded $HEK_{hTRPC6}$ cells were preincubated for 5 min with 2 µM thapsigargin in the presence of various concentrations of larixol (A) or larixyl acetate (B), and then stimulated with ATP (300 µM), carbachol (1 mM), and thrombin (0.5 U/ml) to induce activation of endogenous phospholipase C. Concentration-response curves were fitted to a four parameter Hill equation, and resulting $IC_{50}$ and Hill coefficients are indicated. For comparison, the concentration response curve of TRPC6 inhibition in the OAG-activated mode (Fig. 3D,E of the main manuscript) is superimposed as dashed lines.

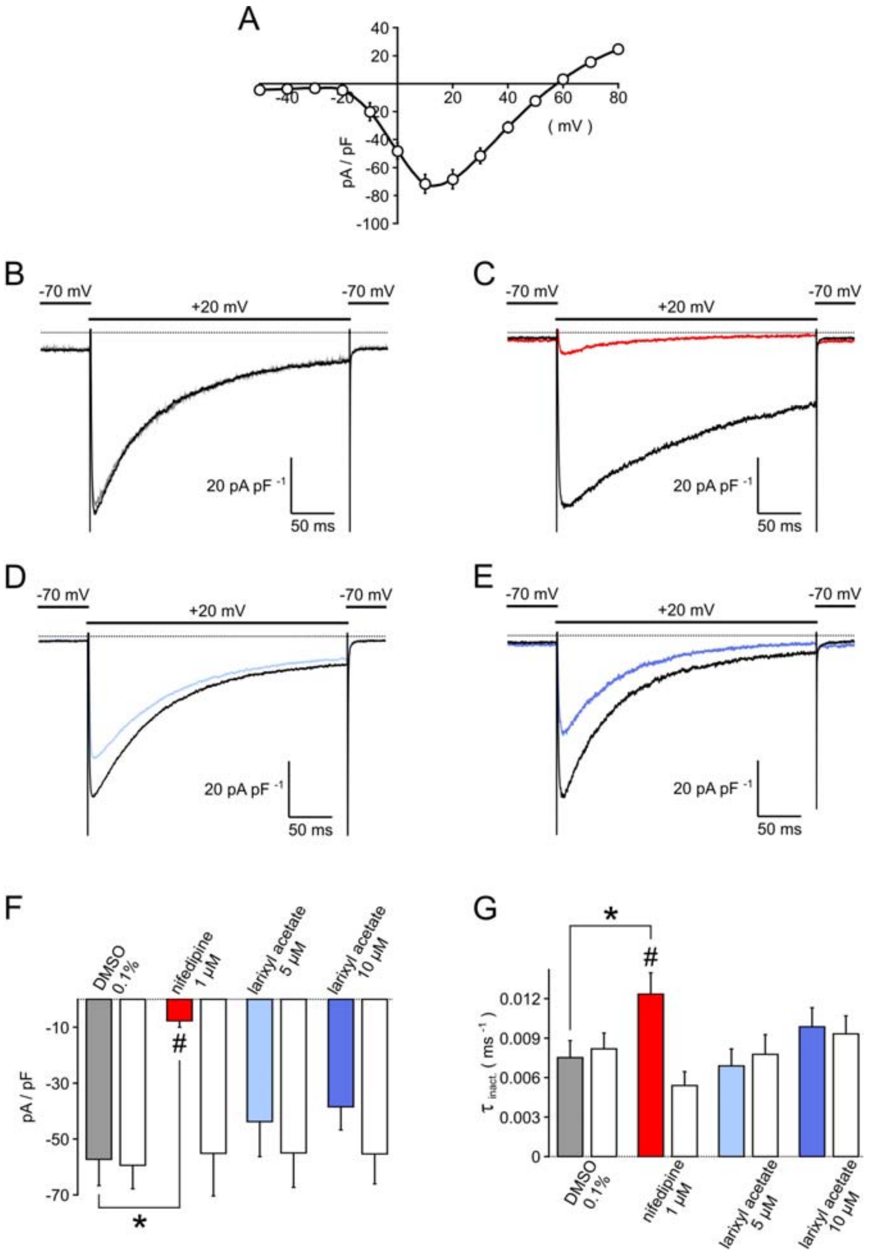


**Supplemental Figure 4: Effect of larixyl acetate on voltage-gated $Ca^{2+}$ channels ($Ca_V1.2$).**

HEK293 cells were transiently transfected with expression plasmids encoding the $\alpha1_{c77}$, the $\beta_{2a}$, and the $\alpha_{2\delta}$ subunits of $Ca_V1.2$ along with a yellow fluorescent protein as transfection marker. (A) $Ba^{2+}$ currents through recombinant $Ca_V1.2$ channels were measured in voltage step protocols, after stepping from a holding potential of -70 mV to the indicated voltages. Shown are means and S.E. of peak current amplitudes determined in 20 patched cells. (B-E) Superposition of depolarisation-induced $Ba^{2+}$ currents in the presence of the indicated modulators, and 160 s after their wash-out (black lines). (F,G) Statistical analysis of modulator effects on peak current densities (F) and on inactivation time constants $\tau_{inact.}$ (monoexponential fits; G) calculated from 6-9 experiments performed as shown in (B-E). Filled bars: values in the presence of the indicated modulators; open bars: values after wash-out of the respective modulator.